

## On the Origin of the Plateau in Surface-Pressure Isotherms of Aromatic Carboxylic Acids

Marysílvia Ferreira,<sup>†</sup> Patrycja Dynarowicz-Łątka,<sup>‡</sup> José Miñones, Jr.,<sup>§</sup> Wilker Caetano,<sup>||</sup> Katarzyna Kita,<sup>‡</sup> Manfred Schálke,<sup>⊥</sup> Mathias Lösche,<sup>⊥</sup> and Osvaldo N. Oliveira, Jr.<sup>\*,#</sup>

Universidade Federal, PEMM-COPPE, Rio de Janeiro, RJ, Brazil, Jagiellonian University, Faculty of Chemistry, Kraków, Poland, Universidad de Santiago de Compostela, Facultad de Farmacia, 15-706 Santiago de Compostela, Spain, Universidade de São Paulo, Instituto de Química de São Carlos and Instituto de Física de São Carlos, São Carlos, SP, Brazil, and Universität Leipzig, Institut für Experimentelle Physik I, Leipzig, Germany

Received: October 3, 2001; In Final Form: March 5, 2002

Langmuir monolayers of 4'-(4-methylphenyl)-5'-phenyl-1,1':3',1''-terphenyl-4-carboxylic acid (*p*-tolyl-PTCA) show a well-defined surface isotherm indicative of a fluid phase followed by a pronounced and broad plateau in which the molecular area decreases by about a factor of 2. The origin of this plateau has been investigated using fluorescence and Brewster angle microscopy (BAM) as well as Fourier transform infrared reflection–absorption spectroscopy (FT-IRRAS). Whereas the surface structure is monomolecular at pressures below the onset of the plateau, the experimental results point to the formation of structures that are no longer monomolecular in the plateau region: As the plateau is reached, changes in the film structure are observed in fluorescence micrographs whereas FT-IRRAS indicates a change in the hydration of the carboxyl groups. A 4-fold increase in reflectivity observed in BAM across the plateau corresponds to an increase in film thickness by a factor of 2. This may correspond to the formation of a laterally homogeneous double layer or to a surface structure that is inhomogeneous on a submicrometer length scale, in which monolayer regions coexist with areas covered with more than two monolayers of material. Subsidiary AFM results indicate the presence of triple-layer patches scattered randomly over a smooth monolayer along the plateau. This is in contradiction to the earlier hypothesis of molecular tilting, which was thought to be more probable than a multilayer formation (Dynarowicz-Łątka, P.; Dhanabalan, A.; Cavalli, A.; Oliveira, O. N., Jr. *J. Phys. Chem. B* 2000, 104, 1701). It thus appears that although polyphenyl carboxylic acids (PTCA and its derivatives) do not show liquid crystalline properties their surface structure resembles more closely that of molecular mesogen films rather than that of monolayers formed by conventional amphiphilic compounds.

## I. Introduction

Monomolecular surface films—so-called Langmuir monolayers—of amphiphilic molecules, such as linear alkanes with a hydrophilic headgroup or biological compounds that possess multiple aliphatic chains, on the surface of water have been intensively investigated in the past.<sup>1–3</sup> Amphiphilic mesogens, containing either rigid or flexible polyaromatic rings, usually modified with aliphatic chains, may form related systems that, however, have been frequently observed to form well-defined and reversible multilayer structures on top of aqueous surfaces.<sup>4,5</sup> In terms of thermodynamics, there exist close relations between these two classes of systems, and in particular, a close analogy between the phase behavior and phase structures of lipid monolayers and mesogen multilayer films has been established.<sup>3,6,7</sup>

In recent work, we have characterized a family of aromatic (polyphenyl) carboxylic acids,<sup>8–12</sup> which are aromatic analogues of the well-investigated aliphatic (polymethylene) amphiphiles extensively explored in Langmuir monolayers<sup>13</sup> and exploited

in Langmuir–Blodgett films.<sup>14</sup> The objective of such work is 2-fold: On one hand, structural information may be inferred from monolayer characterization in comparison with their aliphatic analogues. On the other hand, such compounds may display interesting electron transport and optical properties owing to their  $\pi$  electron systems if order may be established in such systems at the molecular level. An interesting feature in the surface pressure/area ( $\pi$ – $A$ ) isotherms of the investigated aromatic carboxylic acid—5'-phenyl-1,1':3',1''-terphenyl-4-carboxylic acid (PTCA)—and its derivatives is a plateau with an ~50% decrease in area, after which the surface pressure increases again sharply upon compression. An order–disorder transition driven by the van der Waals interactions among the hydrophobic moieties, which is the origin of the LE/LC phase transition in insoluble monolayers of classical amphiphiles,<sup>2</sup> may be ruled out owing to the rigidity of the terphenyl moieties that constitute the hydrophobic surface anchors within the amphiphiles investigated in this study. Thus, generally two alternate interpretations of such a feature lend themselves for an explanation: a transformation of the monomolecular surface layer into a three-dimensional (3D) structure or a collective reorientation of the constituent molecules within the monolayer.<sup>10</sup> From surface potential ( $\Delta V$ – $A$ ) isotherms and  $\Delta V$  measurements on deposited LB films, and in view of the high reproducibility of the  $\pi$ – $A$  isotherms, molecular reorientation was postulated to be the most likely cause for the plateau:<sup>11,12</sup> PTCA was thought

\* Corresponding author. E-mail: chu@if.sc.usp.br.

<sup>†</sup> Universidade Federal.

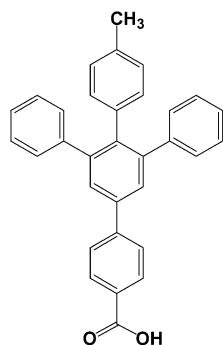
<sup>‡</sup> Jagiellonian University.

<sup>§</sup> Universidad de Santiago de Compostela.

<sup>||</sup> Universidade de São Paulo, Instituto de Química de São Carlos.

<sup>⊥</sup> Universität Leipzig.

<sup>#</sup> Universidade de São Paulo, Instituto de Física de São Carlos.

**CHART 1: Chemical Structure of *p*-tolyl-PTCA**

to tilt over upon compression of the film from an upright into an interdigitated, inclined orientation. Such a collective reorganization was found to account quantitatively for the observed reduction of  $\Delta V$  because the projection of the molecular dipole moment on the surface normal would decrease. An increase in the 2D molecular density through staggering of the molecular moieties was held responsible for the observed area reduction during the transition.<sup>11</sup> The formation of non-monomolecular structures was previously thought to take place only after the midpoint of the plateau, where stripes were observed to form in BAM images.<sup>10,11</sup>

A problem with this interpretation arose from the quantification of the molecular area,  $A$ . The persistence of a monolayer up to the most condensed region, where the measured film area corresponds to  $A \approx 20 \text{ \AA}^2$  per molecule under the assumption of a monomolecular surface film, could be immediately ruled out owing to the physical dimensions of the aromatic ring systems. But even at the beginning of the plateau, which starts at  $A \approx 40 \text{ \AA}^2$ , this area was close to a minimum size that might conceivably accommodate the bulky aromatic rings. We have therefore revisited the problem and have broadened the spectrum of applied experimental techniques. The aim is a better quantification of the surface film thickness by using quantitative Brewster angle reflection measurements and an assessment of intermolecular interactions by using surface-sensitive IR spectroscopy (Fourier transform infrared reflection-absorption spectroscopy, FT-IRRAS). For this study, we selected *p*-tolyl-PTCA (cf. Chart 1) because of the relatively high stability of its monolayers.

## II. Experimental Details

4'-(4-Methylphenyl)-5'-phenyl-1,1':3',1''-terphenyl-4-carboxylic acid (*p*-tolyl-PTCA) was synthesized as described.<sup>8,15</sup> Ultrapure water was used as the subphase for Langmuir monolayers, prepared by spreading aliquots ( $\sim 150 \text{ \mu L}$ ) of a chloroform (Merck, p.a.) solution (concentration  $\approx 0.5 \text{ mg/mL}$ ) onto the air/water interface. Purified  $\text{H}_2\text{O}$  was supplied by a Milli-RO/Milli-Q system (Millipore; resistivity  $> 18 \text{ M}\Omega \text{ cm}$ , pH 5.6–5.8).  $\text{D}_2\text{O}$  was distilled three times in an all-quartz/PTFE (Teflon) apparatus (Normag, Hofheim/Ts., Germany). Surface pressure–area ( $\pi$ – $A$ ) isotherms were measured in a computer-controlled LB film balance (KSV Instruments, Helsinki, Finland, model 5000). After spreading, solvent evaporation was allowed for 5 min before compression was started. Measurements were performed at room temperature.

**II.1. Brewster Angle Microscopy (BAM).** A BAM 2 plus (NFT, Göttingen, Germany) Brewster angle microscope mounted on a Nima, UK trough equipped with a 30-mW laser emitting *p*-polarized light at a wavelength of  $\lambda \approx 690 \text{ nm}$ , was used to visualize the lateral structure of the monolayers as the light beam

is reflected off the air–water interface at the Brewster angle. The shutter speed was 1/1000. The full dependence of the reflected intensity as a function of instrumental settings, film thickness, and optical constants has been given by Berreman.<sup>16</sup> Because we are interested in the transformation of a monolayer into more complex surface film structures, it is sufficient to quantify relative thickness changes. Hence, a simplified approach to data evaluation was taken,<sup>17</sup> which uses the fact that the intensity  $I$  reflected from an optically isotropic molecular film at the Brewster angle of the substrate depends on the film thickness  $d$  as<sup>18</sup>

$$I = Cd^2 \quad (1)$$

where  $C$  is an instrument constant. For a quantification, the gray level output of the camera was converted into absolute intensity values after a calibration that was performed as described by Rodríguez Patino and co-workers.<sup>17</sup>

**II.2. Fluorescence Microscopy.** Fluorescence images were taken with a Nikon Eclipse E800 microscope placed over a small custom-made dual-barrier Langmuir trough with a total area of  $78 \text{ cm}^2$ . Fluorescence was excited with a high-pressure Hg lamp (Nikon). A spectral range of  $\lambda = 580 \pm 14 \text{ nm}$  was selected while the emitted light was detected in a range of  $630 \pm 15 \text{ nm}$  (Nikon filter set MP 5716). A Nikon 20x objective lens was used, resulting in a field of view of size  $640 \text{ \mu m} \times 480 \text{ \mu m}$ . For surface-film visualization, 1 mol % of dipalmitoylphosphatidylethanolamine headgroup-labeled with Texas Red (TR-DPPE, Molecular Probes, Eugene, OR, cat. no. T1395) was admixed to the PTCA solution prior to spreading.

**II.3. Infrared Spectroscopy (FT-IRRAS).** FT-IRRAS measurements were carried out on a BioRad (Digilab) FTS-60A spectrometer. Entering the sample chamber from the external port of the spectrometer, the IR beam is focused with a  $\text{BaF}_2$  lens (focal length, 100 mm) and directed to the water surface with a planar Al mirror at an incident angle of  $\sim 30^\circ$ . After passing a second planar mirror, the reflected beam is focused on a liquid  $\text{N}_2$ -cooled MCT detector using a gold-coated off-axis parabolic mirror. The sample setup consisted of a custom-built thermostated Langmuir trough ( $8 \times 20 \text{ cm}^2$ ) mounted on a shuttle device<sup>19</sup> together with a second trough containing water with a clean surface from which reference spectra were taken. This allows the IR beam to be switched between the sample and reference area without opening the chamber that holds the entire experimental setup, which aids in keeping the humidity constant. *p*-Tolyl-PTCA monolayers were spread at  $20^\circ \text{C}$  on pure water,  $\text{H}_2\text{O}$  or  $\text{D}_2\text{O}$ , and on acidic subphases (pH = 3 adjusted using HCl) or subphases that contained  $10^{-3} \text{ M CaCl}_2$ . Spectra were coadded from 1024 single scans with  $4 \text{ cm}^{-1}$  resolution, apodized with a triangular function, and Fourier transformed with one level of zero filling. Water subphase and vapor rotation–vibration bands were compensated for by subtracting the reference from the sample spectrum.

**II.4. Atomic Force Microscopy (AFM).** Subsidiary experiments were carried out with atomic force microscopy (AFM) using a NanoScope III (Digital Instruments) operating in the contact mode for monolayers of parent PTCA transferred onto silicon and mica. The one-layer LB films from PTCA were transferred from a diluted HCl aqueous subphase (0.001 M) using a NIMA LB trough, with a dipping speed of  $55 \text{ mm/min}$ . Freshly cleaved mica was used without further preparation, whereas silicon wafers had been immersed in Purana cleaning solution ( $\text{H}_2\text{SO}_4/\text{H}_2\text{O}_2$ , 70:30 v/v) for 24 h and then rinsed with water and dried at room temperature. A single layer was transferred in each case, at surface pressure values corresponding

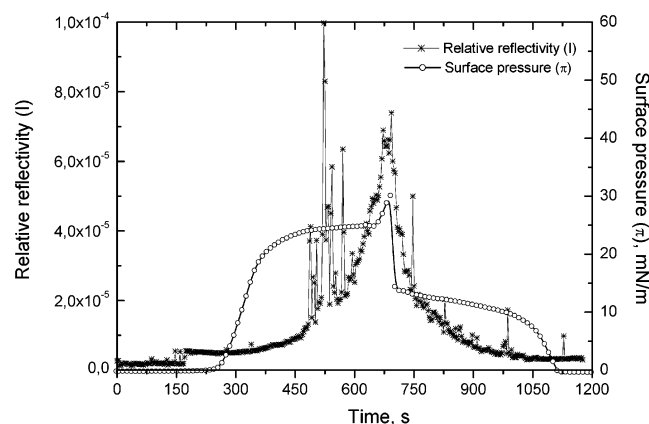


**Figure 1.** Time evolution of the surface pressure  $\pi$  (—○—) and relative reflection intensity (—▽—) during a compression/expansion cycle for *p*-tolyl-PTCA on H<sub>2</sub>O compressed with a speed of  $\sim 7.2 \text{ \AA}^2/(\text{molecule} \times \text{min})$ .

to distinct Langmuir film phases (i.e., in preplateau, plateau, and postplateau regions in the pressure–area isotherm). After the film deposition, the samples were dried at room temperature for 24 h and were further subjected to AFM analysis.

### III. Results and Discussion

In an earlier investigation, we concluded from BAM observations that the PTCA monolayers remain homogeneous upon compression until midplateau, where large-scale folding of the surface structure occurs.<sup>10</sup> Because the resolution of the method is limited to (a few) micrometers, the assessment of “homogeneity” was coupled to that length scale. In the extended work reported here, we use a more quantitative approach, by following the reflection intensity as a function of surface area, to characterize the surface topology upon surface-layer compression. Such a dependence is depicted in Figure 1 for both compression and expansion of a PTCA surface layer. The data show clearly that the reflection intensity is essentially constant during the first steep rise in surface pressure and starts to increase significantly as soon as the plateau is reached. In quantitative terms, the reflectivity increases from  $\sim 1.2 \times 10^{-5}$  to  $\sim 4.9 \times 10^{-5}$  (arbitrary units) across the plateau. At around midplateau, large fluctuations of the reflectivity set in, which indicates the formation of large-scale (mm) inhomogeneities of the surface texture, similar to those observed in previous work.<sup>10</sup> According to eq 1, the observed 4-fold increase in reflection intensity across the plateau indicates an (average) increase in surface-layer thickness by a factor of 2. Whether this corresponds to the formation of a laterally homogeneous double layer or to a surface structure that is inhomogeneous on a submicrometer length scale, in which monolayer areas coexist with areas covered with more than two monolayers of material, cannot be inferred from these data. As evidenced in the second half of the time sequence ( $t > 600 \text{ s}$ ), there is a surface-pressure hysteresis at the onset of the plateau upon decompression; however, the transformation of the surface morphology is perfectly reversible upon expansion, as evidenced by the course of the reflection intensity. If the surface film is allowed to relax for 20 min or more, subsequent compression–decompression cycles lead to essentially identical results.

The appearance of triple-layer patches was inferred from AFM pictures of single-layer LB films from parent PTCA transferred onto mica and silicon wafers. Data on parent PTCA are presented because a systematic study was performed for this compound, whose pressure–area isotherms display similar

features to those of the *p*-tolyl-PTCA compound. Therefore, we believe that the conclusions reached for parent PTCA may be extended to *p*-tolyl-PTCA. Figure 2a shows that at 10 mN/m a homogeneous PTCA monolayer is transferred onto a mica substrate. Upon further film compression, namely, in the midplateau region, double-layered, circular structures are built up on top of a monolayer, as shown in Figure 2b. The vertical dimension of a PTCA molecule is approximately 13–14 Å, according to molecular modeling using HyperChem software. The domains’ heights, being ca. 27 Å, correspond well to a double-layer arrangement. At the plateau termination, the domains become more condensed and increase in height up to 37 Å (Figure 2c). In this region, the domains’ interior is double-layered, whereas their periphery, and especially the points in which the domains adjoin, is much higher. As the film is compressed to the postplateau region (Figure 2d), the transferred films possess multilayer structures typical of collapsed films. Similar results were obtained for PTCA films transferred onto silicon wafers. These AFM results rule out the possibility of a homogeneous double layer for the plateau in the pressure–area isotherm.

In connection with a suitable fluorescent marker, fluorescence microscopy may be a more sensitive means than BAM to characterize lateral homogeneity within the surface films. As judged from isotherms, TR-DPPE did not affect the thermodynamic properties of the surface films, causing merely a slight elevation in the plateau pressure. As shown in Figure 4, of all regimes within the surface isotherm (Figure 3), only the one characterized by the first steep increase in surface pressure is truly homogeneous on the optical length scale (Figure 4b). Whereas at low pressure (Figure 4a) foam structures<sup>20</sup> appear, the surface film shows striped variations in fluorescence intensity as the plateau is entered (Figure 4c). After midplateau (Figure 4d–f), large-scale irregular stripe structures with vast contrast are consistent with the earlier BAM data.<sup>10</sup>

A more detailed assessment of surface-film organization is revealed from IR spectroscopy. Figure 5 shows FT-IRRAS spectra of *p*-tolyl-PTCA at various stages of monolayer compression both on H<sub>2</sub>O (main panel) and on D<sub>2</sub>O subphases (inset). The observed peaks are listed in Table 1, with some of them assigned to specific modes. Whereas the prominent feature around 1670 cm<sup>−1</sup> is connected with a strong index dispersion of the H<sub>2</sub>O subphase<sup>21</sup> and conceals partially the  $\nu(\text{C}=\text{O})$  vibrations and a band near 1600 cm<sup>−1</sup> (cf. inset), a number of other peaks are more clearly identified in the H<sub>2</sub>O spectra, including bands at 1105/1115, 1180, 1240 (shoulder)/1270/1290, 1315, 1370, 1390, and 1410 (shoulder)/1425 cm<sup>−1</sup>. The prominent absorption bands at 1290 and 1425 cm<sup>−1</sup> incorporate major contributions from the carbonyl stretch vibration,  $\nu(\text{C}=\text{O})$ ,<sup>22</sup> which is coupled with the carboxyl OH in-plane bending vibration,  $\delta(\text{COH})$ .<sup>23</sup> IR spectra of various terphenyl mesogens with different substituents attached to their conjugated systems exhibit absorption bands near 1100, 1170, 1235/1280 (with weak intensity of the 1280 cm<sup>−1</sup> band), 1370, 1400/1435, and 1570/1600 cm<sup>−1</sup> (Blume, A., unpublished results) such that an assignment of the PTCA absorption bands near 1110, 1180, and 1370 cm<sup>−1</sup> as characteristic ring vibrations appears likely. In addition, the weak shoulder near 1240 cm<sup>−1</sup> and contributions to the intensity centered at 1270 cm<sup>−1</sup> may be derived from the same origin. For most of these bands, this tentative assignment is backed by Raman spectroscopic and quantum chemical studies of *p*-terphenyl.<sup>24</sup> These show strong C–C stretch vibrations at 1275, 1595, and 1605 cm<sup>−1</sup> that have been, respectively, assigned to normal modes involving the C<sub>4</sub>–C<sub>7</sub>, C<sub>2</sub>–C<sub>3</sub>, and



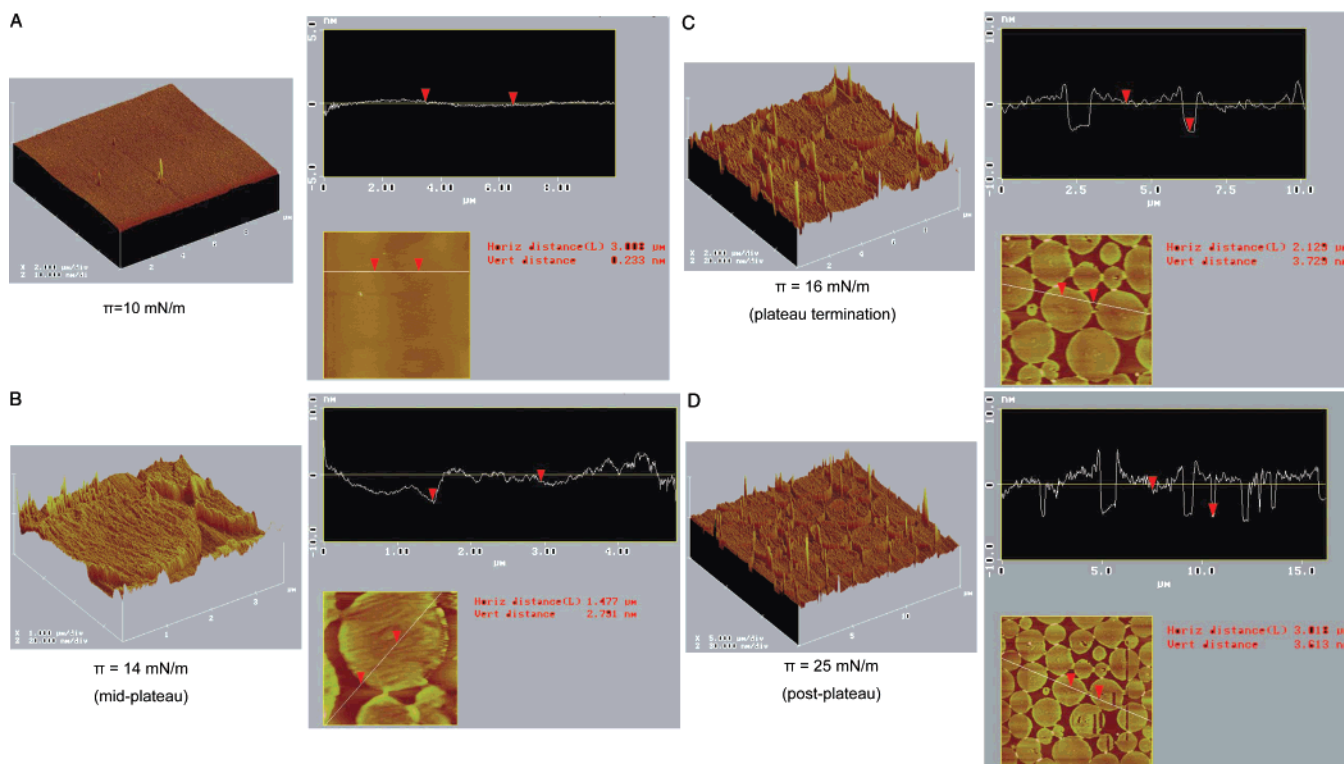


**Figure 2.** AFM pictures and height profiles for a single-layer LB film from PTCA transferred onto a mica substrate at distinct surface pressures: (a) 10 mN/m, (b) 14 mN/m, (c) 16 mN/m, and (d) 25 mN/m.

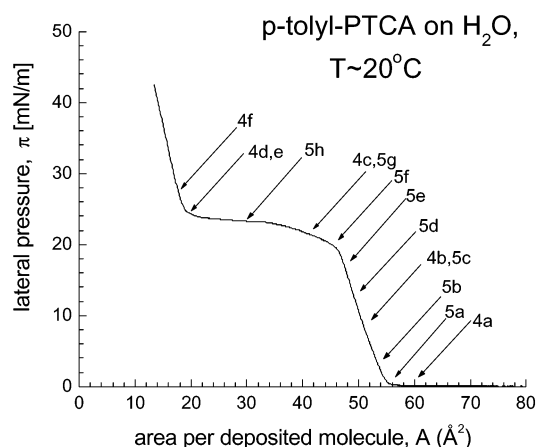


**Figure 3.** Room-temperature isotherm of *p*-tolyl-PTCA containing 1 mol % of TR-DPPE. Indicated are the approximate positions where fluorescence micrographs (Figure 4a–f) and FT-IRRAS spectra (Figure 5a–h) on H<sub>2</sub>O and D<sub>2</sub>O have been obtained.

C<sub>8</sub>–C<sub>9</sub> (and their respective symmetry-related) bonds. These three modes are supposed to have their transition dipole moments oriented parallel to the long axis of the *p*-terphenyl moiety.

As revealed from the IR spectra of D<sub>2</sub>O shown in the inset in Figure 5, there are bands centered at 1610, 1650, 1685, and 1698 cm<sup>-1</sup> that are concealed by the index dispersion due to the H<sub>2</sub>O subphase. Whereas the first of these is presumably associated with the  $\nu(\text{C}_2\text{--C}_3/\text{C}_5\text{--C}_6/\text{C}_{14}\text{--C}_{15}/\text{C}_{17}\text{--C}_{18})$  or  $\nu(\text{C}_8\text{--C}_9/\text{C}_{11}\text{--C}_{12})$  modes of *p*-terphenyl, the bands at 1685 and 1698 cm<sup>-1</sup> are assigned to carbonyl stretch vibrations of the carboxylic acid in various states of protonation. For fatty acids, such a splitting of the  $\nu(\text{C=O})$  mode has been reported between 1704 and 1739 cm<sup>-1</sup>, depending on the subphase pH.<sup>25</sup> Here, substitution with the conjugated system is expected to shift these bands down in energy into the region between 1680 and 1700

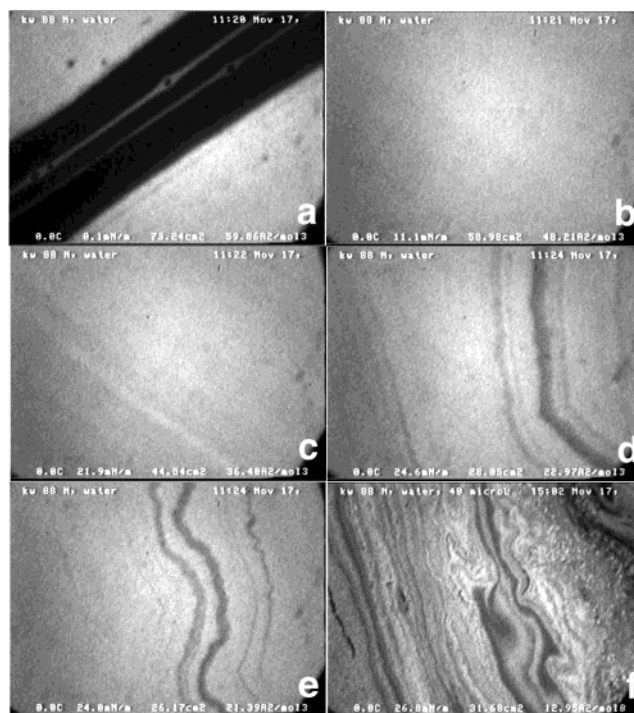


**Figure 4.** Fluorescence micrographs of a *p*-tolyl-PTCA monolayer with 1 mol % TR-DPPE at the positions on the isotherm indicated in Figure 3.

cm<sup>-1</sup>.<sup>22</sup> In addition to the main absorption bands, a number of less-prominent features are observed between 1000 and 1600 cm<sup>-1</sup> as well as between 1700 and 1800 cm<sup>-1</sup> in various groups that incorporate individual peaks with rather regular spacing (cf. Table 1). They have not been assigned. However, PTCA spectra on D<sub>2</sub>O show a very similar pattern of absorption in the 1450 to 1800 cm<sup>-1</sup> region,<sup>1</sup> with the following bands recurring from the H<sub>2</sub>O spectra: 1460, 1515, 1535, 1555, and

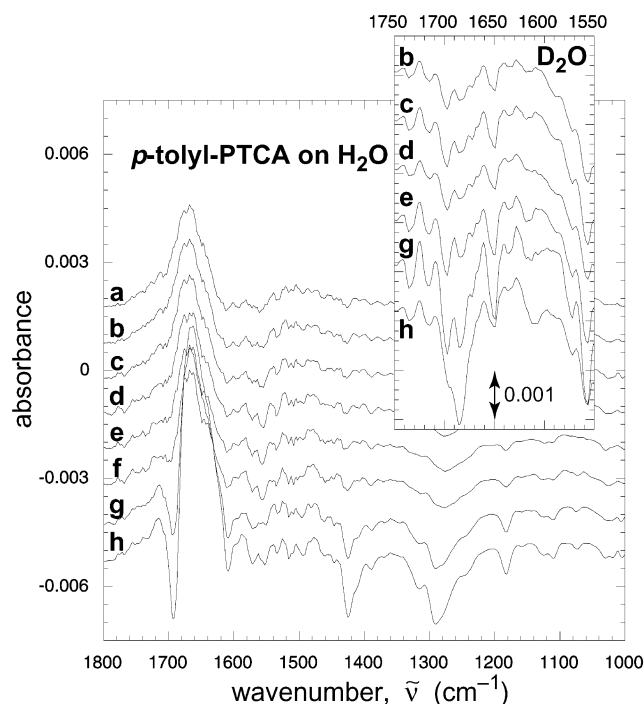


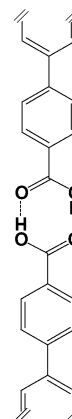
**Figure 5.** FT-IRRAS spectra of *p*-tolyl-PTCA on pure water (main figure: H<sub>2</sub>O; inset: D<sub>2</sub>O) at various surface pressures as indicated in Figure 3. The spectra at the highest pressure on H<sub>2</sub>O and D<sub>2</sub>O were taken at maximum compression such that pressure relaxation during the measurements could not be compensated for. These spectra are hence taken at constant area, not constant pressure.

**TABLE 1: Assignments of FTIR Bands for a *p*-Tolyl-PTCA Monolayer**

wavenumber (cm <sup>-1</sup> )	assignment	symbol	ref
1004, 1019, 1029, 1073	?		
1105/1115	ring vibr	?	[Blume, unpublished]
1180	ring vibr	?	[Blume, unpublished]
1240/1270	ring vibr	$\nu(\text{C}-\text{C})$	24, [Blume, unpublished]
1290	carboxyl stretch + OH bending	$\nu(\text{C}-\text{O})$ $\delta(\text{COH})$	22,23
1315	?		
1370	ring vibr	?	[Blume, unpublished]
1390	?		
1425	carboxyl stretch + OH bending	$\nu(\text{C}-\text{O})$ $\delta(\text{COH})$	22,23
1445, 1460, 1495, 1515, 1535, 1555	?		-
1575	ring vibration	?	[Blume, unpublished]
1610	ring vibration	$\nu(\text{C}-\text{C})$	24, [Blume, unpublished]
1620, 1635, 1650, 1670	?		-
1685/1698/1716	carbonyl stretch di-/mono-/unprotonated	$\nu(\text{C}=\text{O})$	25
1730/1735, 1750, 1770, 1785	?		-

1575 cm<sup>-1</sup>. In the region of the high-energy slope of the H<sub>2</sub>O dispersion, absorption spectra observed on both subphases include bands at 1735, 1750, 1770, and 1785 cm<sup>-1</sup>. From a comparison with calculated vibration frequencies for *p*-terphenyl,<sup>24</sup> it seems reasonable to suggest that many of these features

**CHART 2: Bridging between Two PTCA Molecules that Oppose Each Other, Forming a Double Layer That Exists on Top of a Monolayer**



below 1600 cm<sup>-1</sup> are associated with either  $\nu(\text{C}-\text{C})$  or  $\gamma(\text{C}-\text{C})$  ring modes or else with  $\delta(\text{C}-\text{H})$  deformation modes, all of which are generally calculated to occur in this spectral region. However, none of the vibrations experimentally observed in this work above 1700 cm<sup>-1</sup> are reported in ref 24, such that they are probably a consequence of the more complex ring structure of PTCA as compared to that of *p*-terphenyl.

In the first part of the  $\pi$ -*A* isotherm, where the pressure increases up to  $\pi \approx 20$  mN/m, the spectra are virtually independent of  $\pi$ . This indicates very little change, if any, of molecular orientation or of the hydration of the PTCA's carboxylic acid in the monolayer. Significant changes, however, are observed as the monolayer is compressed into the plateau region: The band centered at 1425 cm<sup>-1</sup>, assigned to  $\nu(\text{C}-\text{O})$  coupled with the COH in-plane bending  $\delta(\text{COH})$ , gains much more intensity than would be expected from a mere increase in molecular density upon compression. Similarly, the band near 1290 cm<sup>-1</sup>, corresponding to the second coupled  $\nu(\text{C}-\text{O})/\delta(\text{COH})$  mode, gains strongly in intensity, surpassing that of the 1270 cm<sup>-1</sup> vibration,  $\nu(\text{C}_4-\text{C}_7/\text{C}_{10}-\text{C}_{13})$ , which prevails at low  $\pi$ .<sup>28</sup> Finally, a similar change in relative intensity is observed on D<sub>2</sub>O for the 1685 and 1698 cm<sup>-1</sup> bands, both associated with  $\nu(\text{C}=\text{O})$  vibrations, albeit at different protonation states. Here the intensity of the band with the lower energy increases much more within the plateau than that of the high-energy band. These observations may be consistently explained if one assumes that the monolayer that exists at lateral pressures below the plateau region is (at least partially) transferred into a multilayer structure in which a significant proportion of the carboxylic headgroups are removed from the water and form interPTCA dimers, as schematically shown in Chart 2. Not only would the carbonyl vibration be expected to shift downward in energy by  $\sim 20$  cm<sup>-1</sup> as the acid undergoes dual protonation but also the carboxyl-dominated bands at 1425 and 1290 cm<sup>-1</sup> will gain more than proportionally in intensity, as quantitatively shown in Figure 6 for the absorption centered at 1425 cm<sup>-1</sup>. Both of these bands have been shown to be particularly strong for dimerized carboxylic acids in an anhydrous environment.

#### IV. Conclusions

We have shown that the plateau in the surface-pressure isotherms of *p*-tolyl-PTCA evolves in response to the formation of multilayer structures. The plateau may not be attributed—at least not entirely—to molecular reorientation, as was previously suggested.<sup>11,12</sup> It is thus revealed that PTCA compounds,

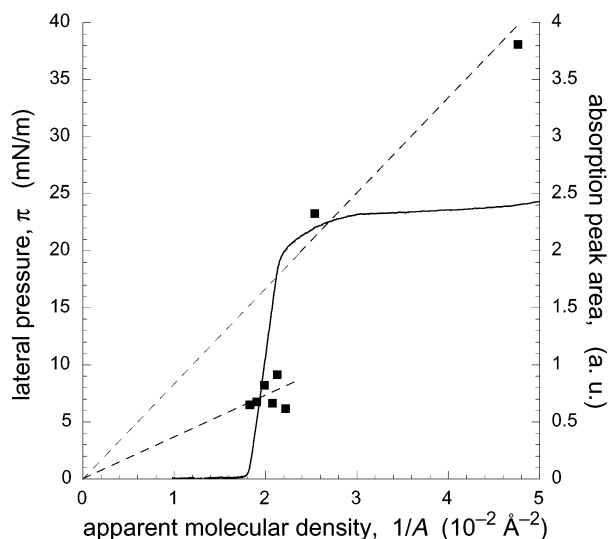


**Figure 6.** Surface pressure  $\pi$  and background-corrected IR absorption at  $1425\text{ cm}^{-1}$  for a *p*-tolyl-PTCA monolayer on  $\text{H}_2\text{O}$  as a function of the apparent molecular area density,  $1/A$ . For the quantitative evaluation of the IR spectra, the range between  $1360$  and  $1460\text{ cm}^{-1}$  has been fitted with four Lorentzian lines (centered approximately at  $1390$ ,  $1410$ ,  $1425$ , and  $1445\text{ cm}^{-1}$ ). Of the results, only the areas underneath the line near  $1425\text{ cm}^{-1}$ , corresponding to the spectrally mixed carboxyl stretch and OH bending modes, have been evaluated and plotted against  $1/A$ . As evident from the plot, the results fall into two distinct groups: (i) Within the range of the first pressure increase and up to the beginning of the plateau, an extrapolation of the data, which are affected by large scattering, toward the origin (— — —) shows a slope that is attributed to an intensity increase due to the compression of one single monolayer at the surface. (ii) After the onset of the plateau, such an extrapolation shows a slope that is approximately twice as large. This shows again that the average molecular density is equivalent to that of two monolayers as the plateau region is reached.

although not exhibiting liquid crystalline properties,<sup>26</sup> are more closely related to mesogenic substances, such as the cyanobiphenyl, 8CB, derivatives studied earlier at the air–water interface.<sup>5,27</sup> For one such compound, an organosiloxane mesogen based on 5CB, a subtle coupling of tilt reorientation and multilayer formation upon surface-film compression, has been demonstrated.<sup>27</sup> For another surface-bound mesogen based on a benzylidenepropylcinnamate, an intriguingly regular sequence of collapse events into subsequently higher orders on  $n$  layers has been reported.<sup>4</sup> A similar well-defined collapse into  $n$  layer structures obviously does not occur with the PTCA system, although the isotherm seems to be consistent with restructuring into a multilayer. The IR results suggest that there occur close contacts between the carboxylic acids of opposing PTCA molecules as soon as the surface film reaches the plateau. This may hint at the formation of triple layers in which the bottom layer is bound to the water surface and is topped by a head-to-head sandwich that maintains hydrophobic contacts both with the bottom layer and with air. Both the isotherm and the ellipsometric thickness measurements as a function of surface area then suggest that this trilayer structure may not be laterally homogeneous within the film area. This conclusion is supported by the fluorescence and Brewster angle microscopy results as well as AFM measurements. In view of the appearance of collapsed domains beyond the midplateau region, however, the

apparent reversibility of the aggregate formation is surprising. Nevertheless, all of the techniques that we have employed show that subsequent compression–decompression cycles lead to results that are very similar to the those in the first cycle.

**Acknowledgment.** We enjoyed fruitful discussions with A. Blume and A. Kerth (Halle, Germany) and are grateful to J. M. Rodríguez Patino (Sevilla, Spain) for making available the BAM system. Fluorescence microscopy has been performed in J. Zasadzinski's laboratory at the University of California, Santa Barbara. We thank FAPESP, CNPq, and Capes (Brazil), the Fulbright Commission, and the DAAD (Germany) for funding.

## References and Notes

- (1) Möhwald, H. *Annu. Rev. Phys. Chem.* **1990**, *41*, 441.
- (2) McConnell, H. M. *Annu. Rev. Phys. Chem.* **1991**, *42*, 171.
- (3) Knobler, C. M.; Desai, R. C. *Annu. Rev. Phys. Chem.* **1992**, *43*, 207.
- (4) Rapp, B.; Gruler, H. *Phys. Rev. A: At., Mol., Opt. Phys.* **1990**, *42*, 2215.
- (5) Schmitz, P.; Gruler, H. *Europhys. Lett.* **1995**, *29*, 451.
- (6) Bibb, A. M.; Knobler, C. M.; Peterson, I. R. *J. Phys. Chem.* **1991**, *95*, 5591.
- (7) Kaganer, V. M.; Möhwald, H.; Dutta, P. *Rev. Mod. Phys.* **1999**, *71*, 779.
- (8) Czapkiewicz, J.; Dynarowicz, P.; Milart, P. *Langmuir* **1996**, *12*, 4966.
- (9) Czapkiewicz, J.; Dynarowicz-Lątka, P.; Janicka, G.; Milart, P. *Colloids Surf., A* **1998**, *135*, 149.
- (10) Dynarowicz-Lątka, P.; Dhanabalan, A.; Oliveira, O. N., Jr. *J. Phys. Chem. B* **1999**, *103*, 5992.
- (11) Dynarowicz-Lątka, P.; Dhanabalan, A.; Cavalli, A.; Oliveira, O. N., Jr. *J. Phys. Chem. B* **2000**, *104*, 1701.
- (12) Dynarowicz-Lątka, P.; Dhanabalan, A.; Oliveira, O. N., Jr. *Langmuir* **2000**, *16*, 4245.
- (13) Möhwald, H. In *Structure and Dynamics of Membranes: From Cells to Vesicles*; Lipowsky, R., Sackmann, E., Ed.; North-Holland: Amsterdam, 1995; Vol. 1A, p 161.
- (14) Kuhn, H.; Möbius, D.; Bücher, H. In *Physical Methods of Chemistry*; Weissberger, A., Rossiter, B. W., Ed.; Wiley: New York, 1972; Vol. I, p 577.
- (15) Dynarowicz-Lątka, P.; Czapkiewicz, J.; Kita, K.; Milart, P.; Broclawik, E. *Prog. Colloid Polym. Sci.* **1999**, *112*, 15.
- (16) Berreman, D. W. *J. Opt. Soc. Am.* **1972**, *62*, 502.
- (17) Rodríguez Patino, J. M.; Sánchez, C. C.; Rodríguez Niño, M. R. *Langmuir* **1999**, *15*, 2484.
- (18) Azzam, R. M. A.; Bashara, N. M. *Ellipsometry and Polarized Light*; North-Holland: Amsterdam, 1992.
- (19) Fitter, J.; Lechner, R. E.; Büldt, G.; Dencher, N. A. *Physica B* **1996**, *226*, 61.
- (20) Lösche, M.; Sackmann, E.; Möhwald, H. *Ber. Bunsen-Ges. Phys. Chem.* **1983**, *87*, 848.
- (21) Blaudez, D.; Buffeteau, T.; Cornut, J. C.; Desbat, B.; Escarfe, N.; Pezolet, M.; Turlet, J. M. *Thin Solid Films* **1994**, *242*, 146.
- (22) Bellamy, L. J. *The Infrared Spectra of Complex Molecules*; Methuen: London, 1958.
- (23) Hadzi, D.; Sheppard, N. *Proc. R. Soc., Ser. A* **1953**, *216*, 247.
- (24) Amorim da Costa, A. M.; Karger, N.; Amado, A. M.; Becucci, M. *Solid State Ionics* **1997**, *97*, 115.
- (25) Gericke, A.; Hühnerfuss, H. *J. Phys. Chem.* **1993**, *97*, 12899.
- (26) Dynarowicz-Lątka, P.; Kita, K.; Milart, P.; Dhanabalan, A.; Cavalli, A.; Oliveira, O. N., Jr. *J. Colloid Interface Sci.* **2001**, *239*, 145.
- (27) Harke, M.; Motschmann, H. R. *Langmuir* **1998**, *14*, 313.
- (28) In contrast, the spectral region around  $1250\text{ cm}^{-1}$  is concealed by the water-index dispersion of  $\text{D}_2\text{O}$  such that a direct comparison of the carboxyl bands on the two subphases is not feasible. We note that both the  $1290$  and  $1425\text{ cm}^{-1}$  bands are expected to shift appreciably—into the ranges around  $1350$  and  $1050\text{ cm}^{-1}$ , respectively.<sup>23</sup> We are not able to confirm clearly the entire absence of these bands at the positions where they are observed on  $\text{H}_2\text{O}$  (there is a small absorption located near  $1420\text{ cm}^{-1}$  on  $\text{D}_2\text{O}$  that grows proportionally to the molecular density of the surface film). Nor do we clearly observe new bands because of the interference of the  $\text{D}_2\text{O}$  dispersion.